



Accepted Article

Title: Quantitative Profiling of the Heavy Atom Effect in BODIPY Dyes:
Correlating Initial Rates, Atomic Numbers and 1O₂ Quantum
Yields

Authors: Yannick Rey, Dario Abradelo, Nico Santschi, Christian
Strassert, and Ryan Gilmour

This manuscript has been accepted after peer review and appears as an Accepted Article online prior to editing, proofing, and formal publication of the final Version of Record (VoR). This work is currently citable by using the Digital Object Identifier (DOI) given below. The VoR will be published online in Early View as soon as possible and may be different to this Accepted Article as a result of editing. Readers should obtain the VoR from the journal website shown below when it is published to ensure accuracy of information. The authors are responsible for the content of this Accepted Article.

To be cited as: *Eur. J. Org. Chem.* 10.1002/ejoc.201601372

Link to VoR: <http://dx.doi.org/10.1002/ejoc.201601372>

Quantitative Profiling of the Heavy Atom Effect in BODIPY Dyes: Correlating Initial Rates, Atomic Numbers and $^1\text{O}_2$ Quantum Yields

Yannick P. Rey,^{a†} Dario G. Abradelo,^{b†} Nico Santschi,^{a†} Cristian A. Strassert,^{b*} and Ryan Gilmour^{a*}

Dedicated to Prof. Dr. Peter H. Seeberger on the occasion of his 50th birthday.

Abstract: Direct oxidation using molecular oxygen is both attractive and atom efficient. However, this first requires catalyst-based activation or electronic reconfiguration of inert O_2 . The most expedient strategy relies on the generation of singlet oxygen ($^1\text{O}_2$; $a^1\Delta_g$) from the triplet state ($^3\text{O}_2$; $X^3\Sigma_g^-$) by a photosensitizer. In the current arsenal of photosensitizers, boron-dipyrromethene (BODIPY) cores are considered privileged on account of their unique photophysical characteristics, and the ability to tune behavior by facile structural modifications such as halogen incorporation (X). Thus the scaffold has become synonymous with the renowned *Heavy Atom Effect* (HAE); a phenomenon that correlates the increasing atomic number (Z_X) of pendant halogen atoms with enhanced probability of intersystem crossing ($S_1 \rightarrow T_1$). Herein, a facile GC-based method to assess catalyst performance has been developed, and validated using a focused set of halogenated BODIPY scaffolds. An initial rate approximation was applied to a model transformation and follows the HAE trend ($v_{0,H} < v_{0,Cl} < v_{0,Br} < v_{0,I}$). This operationally simple approach was corroborated by complementary determination of absolute singlet oxygen and photoluminescent quantum yields and time-resolved luminescence decays to evaluate lifetimes. For double logarithmic plots, linear correlations of relative intersystem crossing rates k_{isc}^X / k_{isc}^Y and relative atomic numbers Z^X / Z^Y for the respective substituents with corresponding slopes of approximately 4 were obtained: $k_{isc} \sim Z^4$, which also was shown to hold for the fluorescence lifetime-corrected singlet oxygen quantum yields as independent measurements. This substantiates theoretical predictions pertaining to the *Heavy Atom Effect*.

both expansive and ubiquitous in chemistry and biology.^[1] Considerations of atom economy,^[2] and the natural abundance of dioxygen, advocate this approach as being both sustainable and facile.^[3] Consequently, the singlet state ($^1\text{O}_2$; $a^1\Delta_g$) has found widespread application, both in therapeutic medicine as a component of photodynamic therapy,^[4] and complex molecule synthesis.^[5] In both scenarios, effective (often organic) photosensitizers are essential to generate reactive singlet oxygen ($^1\text{O}_2$) from its native triplet state ($^3\text{O}_2$). These species mediate energy transfer from excited states as opposed to electron transfer (Figure 1).^[6] In view of the fundamental importance of organic photosensitizers in medicine, together with the rapidly evolving field of organic photocatalysis,^[7] methods to rapidly and quantitatively profile the efficiency of novel architectures are of practical value.

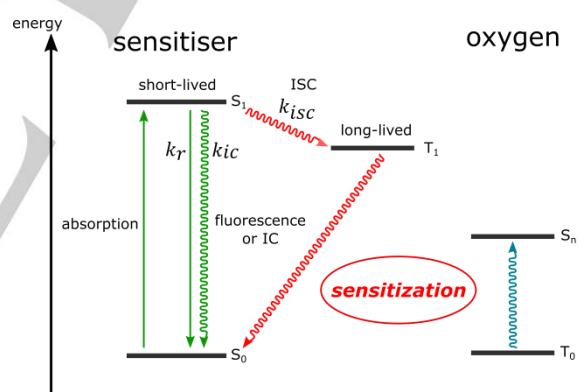


Figure 1. An overview of the photosensitized $^1\text{O}_2$ generation.

Introduction

Unleashing the latent reactivity of molecular oxygen by direct photosensitization to generate its first excited electronic state is

We therefore sought to develop an operationally simple, GC-based comparative analysis of photosensitizing BODIPY fluorophores to circumvent the need for quantum yield determination, and independently validate it by classical photophysical analysis. Since these systems are competent generators of singlet oxygen,^[8] it was envisaged that the reactive $^1\text{O}_2$ produced *in situ* might be intercepted by selected reaction partners, thus allowing for the facile determination of the initial rates (v_0). Systematic halogen exchange at the 2- and 6-positions allows the *Heavy Atom Effect*^{[6][9]} to be exploited to ensure a qualitatively predictably augmentation of intersystem crossing, and by extension, efficiency of $^1\text{O}_2$ generation. Compounds **1-10** were prepared for comparative analysis (Figure 2).^[10] Substitution of the 2- and the 6-positions of the

[a] Dr. Y. P. Rey, Dr. N. Santschi, Prof. Dr. R. Gilmour
Institut für Organische Chemie and Excellence Cluster EXC 1003,
Cells in Motion, Westfälische Wilhelms-Universität Münster
Corrensstrasse 40, 48149 Münster, Germany.
E-mail: ryan.gilmour@uni-muenster.de
Homepage: <http://www.uni-muenster.de/Chemie.oc/gilmour/>

[b] Dr. D. G. Abradelo, Dr. C. A. Strassert
CeNTech, Physikalisches Institut, Westfälische Wilhelms-
Universität, Heisenbergstrasse 11, 48149 Münster, Germany.
E-mail: ca.s@uni-muenster.de

* These authors contributed equally.

Full paper

WILEY-VCH

BODIPY core by halogen atoms of differing atomic number should elicit the following HAE trend in an initial rate analysis:

$$V_{0,H} < V_{0,Cl} < V_{0,Br} < V_{0,I}$$

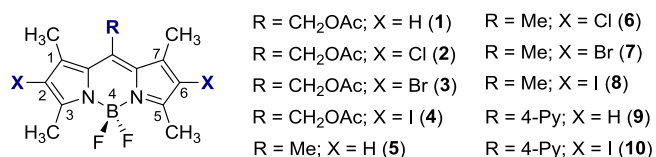


Figure 2. BODIPY dyes 1-10 designed to probe the HAE.

Numerous studies have been published on the synthesis of 2,6-dihalogenated BODIPY dyes,^[11] either as precursors for subsequent functionalization strategies (e.g. cross-coupling chemistry) or in order to increase the rate of intersystem crossing (k_{isc}). Typically, the onset of the latter manifests itself in a notably decreased fluorescence quantum yield (Φ_F) and lifetime (τ) and may, concomitantly, lead to a significantly enhanced singlet oxygen quantum yield (Φ_Δ)^[12] – a property highly desirable for applications in photodynamic therapy (PDT). However, this correlation is of a qualitative nature. Generally, intersystem crossing is influenced by spin-orbit coupling (SOC). Specifically, SOC is dependent on Z^4 , where Z denotes the atomic number of the halogen substituent. In turn, the rate of intersystem crossing (k_{isc}) should display the same dependency ($k_{isc} \sim Z^4$). To the best of our knowledge, this quantitative description of the HAE in 2,6-dihalogenated BODIPY chromophores has not been reported.^[13]

Herein, we demonstrate that for two different *meso*-substituents (R = CH₃, CH₂OAc & X = Cl, Br or I) k_{isc} as well as fluorescence lifetime-corrected Φ_Δ correlate strongly with Z^4 , thereby corroborating the presence of a HAE in halogenated BODIPY chromophores and demonstrating the suitability of an operationally trivial, GC-based initial rate analysis for comparative analysis of photosensitizers. The conceptual framework of this profiling approach is summarized in Figure 3. In order to develop a simple method for the rapid and qualitative identification of highly efficient oxygen sensitization chromophores, a library constituting of 10 different BODIPY derivatives was prepared (Figure 2). Three core architectures featuring varying *meso*-substituents were further modified by *bis*-halogenation in the 2- and 6-position, thereby gradually activating an internal heavy atom effect.

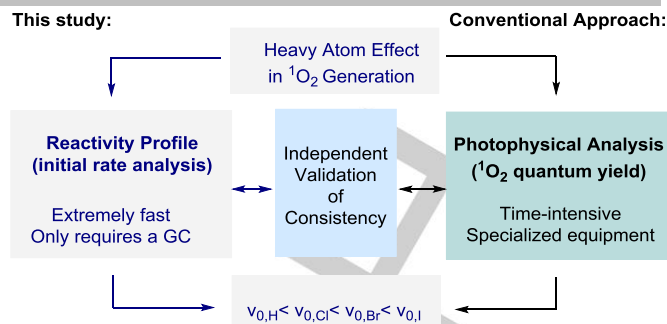


Figure 3. Conceptual approach to ¹O₂ photosensitizer profiling: Integrating reactivity (v_0) and photophysical (Φ_Δ and Φ_F) descriptions.

Results and Discussion

Prior to the initial rate analysis, a more detailed photophysical analysis of compounds 1-10 was performed beginning with characterization by absorption spectroscopy: These results are summarized in the Supporting Information. Fluorescence excitation and emission spectra were also acquired in solution and in frozen CH₂Cl₂/MeOH 1:1 glassy matrices kept at 77 K under liquid nitrogen in calibrated quartz-Dewars. Furthermore, absolute photoluminescent quantum yields (Φ_F) and time-resolved luminescence decays were determined to evaluate lifetimes and create a full description of the photocatalysts for the ensuing comparison with initial rate behavior. The absorption excitation, and emission spectra as well as the luminescence decay curves of each compound are depicted in the Supporting Information, together with the relevant photophysical data including Φ_F , radiative and non-radiative rate constants. A summary of the most relevant photophysical data is presented in Table 1. Values of the radiative and non-radiative constants were calculated according to equations 1 and 2, which consider the common deactivation pathways of the S1 excited state (Fig. 1).

Table 1. Lifetime and absolute Φ_F values, together with the correspondent radiative and non-radiative constants of sensitizers 1–10 at room temperature (r.t.) and 77 K.^[a]

Sensitizer	$\tau_{S1}^{[b]}$ (ns), r.t.	Φ_F r.t. ^[c]	k_r r.t. (s ⁻¹)/10 ⁸	k_{nr} r.t. (s ⁻¹)/10 ⁸	τ_{S1} 77K ^[b] (ns)	Φ_F 77K ^[c]	k_r 77K (s ⁻¹)/10 ⁸	k_{nr} 77K (s ⁻¹)/10 ⁸
1	6.59	0.74	1.12 ± 0.06	0.40 ± 0.02	6.47	1.00	1.51 ± 0.04	< 0.08
2	6.20	0.60	0.97 ± 0.05	0.65 ± 0.03	6.76	1.00	1.44 ± 0.04	< 0.07
3	1.95	0.16	0.82 ± 0.04	4.3 ± 0.2	3.39	0.49	1.43 ± 0.07	1.52 ± 0.07
4	0.25	0.02	0.85 ± 0.04	40 ± 2	0.56	0.06	1.07 ± 0.06	16.79 ± 0.05
5	7.62	0.85	1.11 ± 0.06	0.20 ± 0.01	5.28	0.99	1.81 ± 0.05	< 0.11
6	5.89	0.74	1.26 ± 0.06	0.44 ± 0.02	5.91	1.00	1.64 ± 0.04	< 0.09
7	2.10	0.23	1.08 ± 0.05	3.7 ± 0.2	3.15	0.48	1.53 ± 0.07	1.64 ± 0.08
8	0.33 ^[d]	0.03	0.81 ± 0.04	29 ± 2	0.63 ^[b]	0.08	1.19 ± 0.06	14.66 ± 0.06
9	1.62	0.16	1.00 ± 0.05	5.2 ± 0.3	5.68	1.00	1.72 ± 0.04	< 0.09
10	0.22 ^[d]	0.01	0.57 ± 0.03	45 ± 2	0.52 ^[b]	0.06	1.11 ± 0.05	18.3 ± 0.1

^[a] DCM and a mixture of DCM/MeOH 1:1 were used for the measurements at r.t. and 77 K respectively. ^[b] ±0.05^[c] ±0.02. ^[d] Lifetimes were not mono-exponential, component with the highest fractional contribution reported.

$$k_r = \frac{\Phi_F}{\tau} \quad (1)$$

$$k_{nr} = k_{ic} + k_{isc} = \frac{1-\Phi_F}{\tau} \quad (2)$$

In order to account for the HAE, the generally accepted notion that intersystem crossing is favored by spin-orbit coupling (SOC) was considered.^[14] The energy involved in spin-orbit splitting is described by solution of Dirac's relativistic wave equation,^[15] and has a direct proportionality to Z^4 , where Z is the atomic number, in this case of the halogen. A direct dependence between the intersystem crossing rate constant (k_{isc}) and Z^4 is expected (i.e. $k_{isc} \sim Z^4$) and has been reported by several authors to account for the HAE.^[16] However, the direct determination of k_{isc} is often hampered by the concomitant occurrence of other non-radiative processes such as internal conversion (Scheme 1). To circumvent this problem, it was assumed that vibrational, rotational or collisional deactivation of the S_1 state is negligible in frozen matrices ($T = 77$ K), where $k_{isc} = k_{nr}^{77K}$. The latter is generalized in equation 3 and describes any pair of heavy atoms X and Y in equation 4.

$$k_{nr X}^{77K} \cong k_{isc X} \propto Z_X^4 \quad (3)$$

$$\ln\left(\frac{k_{nr X}^{77K}}{k_{nr Y}^{77K}}\right) = 4 \cdot \ln\left(\frac{Z_X}{Z_Y}\right) \quad (4)$$

Figure 4 shows the correlation obtained with equation 4 for two series of sensitizers, e.g. **2-4** with $R = \text{CH}_2\text{OAc}$ and **6-8** with $R = \text{CH}_3$. The slope values were 4.7 ± 0.4 and 4.4 ± 0.3 for $R = \text{CH}_2\text{OAc}$ and CH_3 , respectively, and near four in both cases which support the validity of the photophysical model proposed. BODIPY molecules substituted with H, i.e. **1** and **5**, are not represented due to the large deviation in the correlation observed for the other compounds, as also reflected by the absorption spectra. The nature of the excited states is different, as no halogen is involved and SOC in these molecules is expected to be negligible (with a Φ_F near 1), which invalidates the use of equation 3.

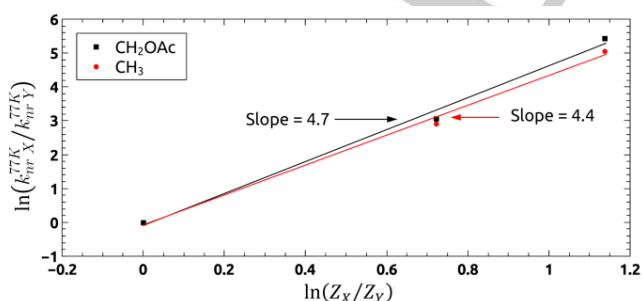


Figure 4. Heavy atom effect dependence of the k_{nr}^{77K} with the atomic number (Z) for the series of sensitizers containing $R = \text{CH}_2\text{OAc}$ and $R = \text{CH}_3$. $X = -\text{I}$, $-\text{Br}$, $-\text{Cl}$; $Y = -\text{Cl}$ (Compounds **2-4**, **6-8**).

Next, photogeneration of $^1\text{O}_2$ was determined by steady state infrared emission spectroscopy (Figure 5), monitoring the phosphorescence intensity of the photosensitized singlet oxygen

as a function of fraction of light absorbed ($1-10^{-A}$). Φ_Δ values were quantitatively determined using equation 5:

$$\Phi_\Delta^S = \Phi_\Delta^R \cdot \frac{m_S}{m_R} \quad (5)$$

where S is the molecule of interest, R is a reference monitor with a known value of Φ_Δ , and m is the slope of the integrated emission vs. the fraction of light absorbed. Tetra-*t*-butylphthalocyaninato zinc(II) (TTB-ZnPc) was used as the reference monitor ($\lambda_{\text{exc}} = 650$ nm, $\Phi_\Delta = 0.62$)^[17] and the intensities were corrected for the power of the excitation beams at each wavelength. The phosphorescence lifetime of singlet oxygen was independent of the sample, and no correction of its phosphorescence intensity was necessitated to account for different quenching pathways that could affect the monitored emission.

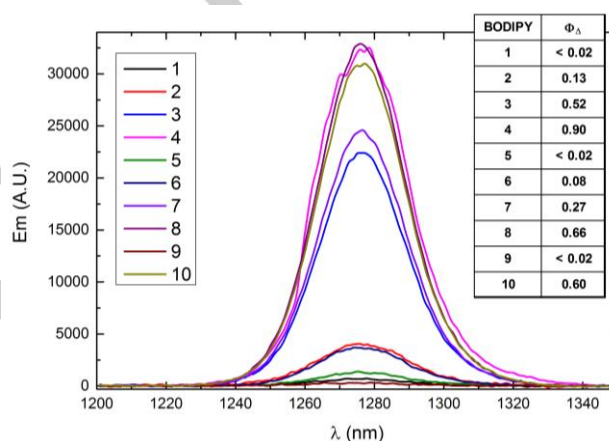


Figure 5. Emission spectra of the singlet oxygen photogenerated by compounds **1-10** in solutions with same absorptivity values. Inset: singlet oxygen quantum yields.

Values of Φ_Δ for compounds **1-10** are depicted in Figure 5 (inset) and reveal the expected HAE, where molecules with $-\text{I}$ (**4**, **8**, **10**) exhibited the highest SO quantum yields, followed by those with $-\text{Br}$ (**3**, **7**), $-\text{Cl}$ (**2**, **6**), and lastly $-\text{H}$ (**1**, **5**, **9**). In order to quantitatively account for these empirical results, equation 6 was used, which led to an expression analogous to equation 4 (equation 7) (assuming that the energy transfer efficiency is independent of the photosensitizer employed, see SI).

$$\frac{k_{isc X}}{k_{isc Y}} \cong \frac{\Phi_\Delta^X \cdot \tau^Y}{\Phi_\Delta^Y \cdot \tau^X} \quad (6)$$

$$\ln\left(\frac{\Phi_\Delta^X \cdot \tau^Y}{\Phi_\Delta^Y \cdot \tau^X}\right) = 4 \cdot \ln\left(\frac{Z_X}{Z_Y}\right) \quad (7)$$

Figure 6 shows the correlation obtained with equation 7 for two series of sensitizers, i.e. those with $R = \text{CH}_2\text{OAc}$ and $R = \text{CH}_3$. The determined slope values were 3.8 ± 0.7 and 3.6 ± 0.9 for $R = \text{CH}_2\text{OAc}$ and CH_3 , respectively, which lends additional support to the validity of the model proposed. It should be noted that the robustly coincident correlations presented in Figures 4 and 6 are the result of completely independent photophysical determinations (different temperatures, matrices, instruments

Full paper

WILEY-VCH

and observables), and pointed to similar results within the experimental uncertainty. Compounds **1**, **5** and **9** did not fall, as expected, in the observed trend.

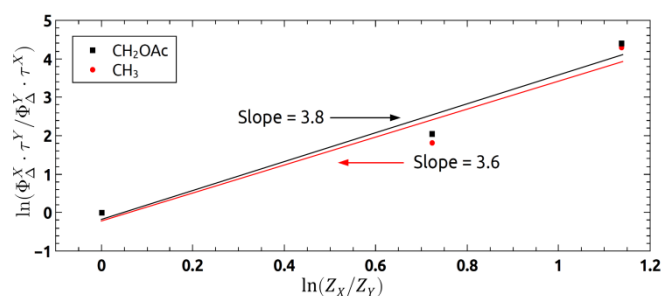
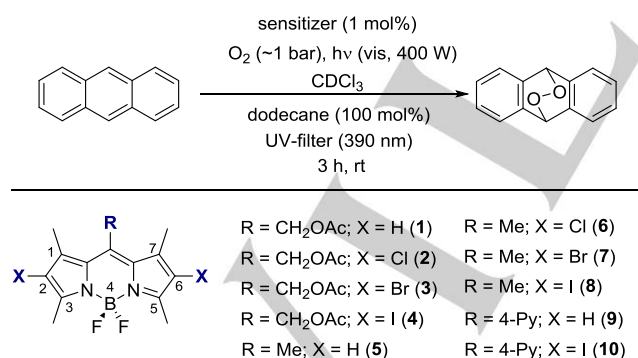


Figure 6. Heavy atom effect dependence of the singlet oxygen photogeneration with the atomic number (Z) for the series of sensitizers containing $R = \text{CH}_2\text{OAc}$ and $R = \text{CH}_3$. $X = -\text{I}, -\text{Br}, -\text{Cl}$; $Y = -\text{Cl}$ (Compounds **2**, **3**, **4**, **6**, **7**, **8**).

With the photophysical characterization completed, attention was then focused on monitoring the efficiency of the BODIPY sensitizers in the generation of $^1\text{O}_2$ without the need of specialized equipment. The simplest strategy is to trap the reactive oxygen as a stable adduct with a second reactant. To that end, the well-known [4+2]-cycloaddition of singlet oxygen and anthracene was chosen due to the formation of a single product that can be easily analysed by gas chromatography (Scheme 2).

All reactions were irradiated for 3 h under an oxygen atmosphere and at a concentration of 0.1 M with respect to anthracene [100 μmol scale using 1 mol% of sensitizer (**1-10**)] (Scheme 1). Dodecane (100 μmol) was added as an internal standard prior to irradiation for accurate determination of the conversion by gas chromatography. Aliquots were taken at regular time intervals.



Scheme 1. Conditions for the photosensitized peroxidation of anthracene using BODIPY structures **1-10** (1 mol% catalyst loading).

In all reactions, a linear dependence of the consumption of anthracene and the reaction time was observed, well beyond 50% conversion (Figure 7). This allowed for facile determination and comparison of the initial rate (v_0) of all transformations using **1-10**. A clear relationship between the initial rates and the substituents on the 2- and 6-positions was observed: As

expected, the heavier the substituent the faster the reaction: $V_{0,\text{H}} < V_{0,\text{Cl}} < V_{0,\text{Br}} < V_{0,\text{I}}$.

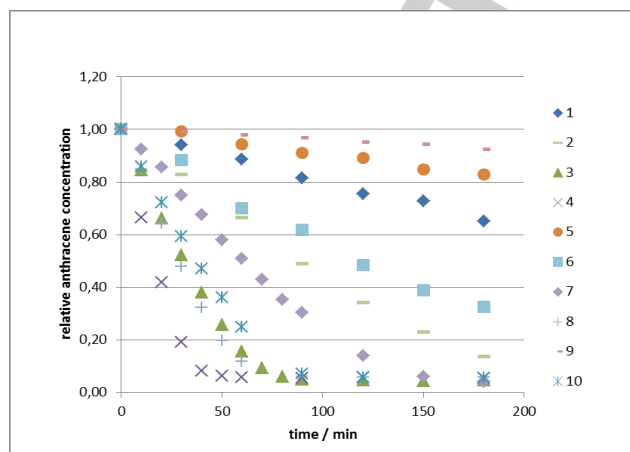


Figure 7. Consumption of anthracene over time using structures **1-10** as sensitizers.

Importantly, this trend holds for three distinct sub-structure classes that vary in the substituent R (CH_2OAc **1-4**, Me **5-8** and 4-Py **9-10**). The consumption of anthracene in the absence of a photosensitizer was also measured as a control. In order to compare the reaction rates quantitatively, the initial rates (over the linear section) of each reaction was determined (Table 2).

Investigation of the parent compound **1** (entries 1 and 2) revealed that even without heavy atoms on positions 2- and 6- the BODIPY structure is capable of generating singlet oxygen, and an initial rate of $3.2 \mu\text{M}\cdot\text{s}^{-1}$ was observed (vs. $0.7 \mu\text{M}\cdot\text{s}^{-1}$ without sensitizer). As expected, halogenation augmented the reaction rates in the order $\text{Cl} < \text{Br} < \text{I}$, consistent with an internal Heavy Atom Effect (entries 3-5; $9.2 \mu\text{M}\cdot\text{s}^{-1}$, $26.0 \mu\text{M}\cdot\text{s}^{-1}$ and $44.6 \mu\text{M}\cdot\text{s}^{-1}$, respectively). Simple $\text{H} \rightarrow \text{I}$ substitution resulted in a significant increase of the initial rate from $3.2 \mu\text{M}\cdot\text{s}^{-1}$ to $44.6 \mu\text{M}\cdot\text{s}^{-1}$ ($\Delta v_{0,\text{H-I}} = 41.4 \mu\text{M}\cdot\text{s}^{-1}$). The expected dependence of the initial rate on the halogen substituents ($\text{Cl} < \text{Br} < \text{I}$) was also observed with the methyl-derived photosensitizers (entries 7-9, $7.2 \mu\text{M}\cdot\text{s}^{-1}$, $13.7 \mu\text{M}\cdot\text{s}^{-1}$ and $28.8 \mu\text{M}\cdot\text{s}^{-1}$, respectively). Importantly, relative to the uncatalyzed reaction, the non-halogenated catalyst **5** only improved the initial rate by a factor of 2.5 (entries 1 and 7, $0.7 \mu\text{M}\cdot\text{s}^{-1}$ vs. $1.7 \mu\text{M}\cdot\text{s}^{-1}$). In this catalyst subclass ($R = \text{Me}$) a smaller rate enhancement was observed upon iodination of the parent structure **5** $\Delta v_{0,\text{H-I}} = 27.1 \mu\text{M}\cdot\text{s}^{-1}$ (compared to $41.4 \mu\text{M}\cdot\text{s}^{-1}$ for $R = \text{CH}_2\text{OAc}$). In general, sensitizers **5-8** proved to be less effective in mediating this transformation compared to their acetoxy analogues **1-4**, but the HAE effect trend holds. According to a report by Caruso *et al.*^[9b] BODIPY structure **10** bearing a 4-pyridyl substituent on the *meso*-position is a highly efficient singlet oxygen generator.

In our hands, the non-halogenated derivative **9** closely mirrored the initial rate behavior of the background reaction. Whilst this behavior clearly changes upon iodination of the 2- and 6-positions ($\text{H} \rightarrow \text{I}$), compound **10** led to the lowest initial rate of the photocatalysts investigated (entry 11, $22.1 \mu\text{M}\cdot\text{s}^{-1}$ cf. entries

Full paper

WILEY-VCH

5 and 9, 44.6 and 28.8 $\mu\text{M}\cdot\text{s}^{-1}$, respectively). Inspection of entries **10** and **11** indicate that in the case of the 4-pyridine derived sensitizers, iodination does lead to an increase of the initial rate from 0.7 $\mu\text{M}\cdot\text{s}^{-1}$ to 22.1 $\mu\text{M}\cdot\text{s}^{-1}$ ($\Delta v_{0,\text{H-I}}=21.4 \mu\text{M}\cdot\text{s}^{-1}$), but this is the smallest increase noted throughout the study.

To corroborate the hypothesis that motivated this study, data obtained from the full photophysical characterization of the photosensitizing BODIPY fluorophores (Φ_F , Φ_Δ) was compared with the GC-based initial rates (v_0). To this end, the initial rates v_0 were transformed to corrected initial rates $v_{0,\text{corr}} = v_0 / \text{CF}$, by calculating a correction factor CF taking into account the overall lamp emissive profile and the chromophores' absorption spectra (for full details see the SI).

Table 2. Initial rates v_0 obtained for BODIPY sensitizers

Entry	Sensitizer	v_0 [M s^{-1}] ^[a]	CF ^[a]	$v_{0,\text{corr}}$ [M s^{-1}] ^[b]	Φ_F (RT)	Φ_Δ
1	None	0.70e-6	-	-	-	-
2	1 (R = OAc)	3.18e-6	0.39	8.16e-6	0.74	0.02
3	2	9.21e-6	0.46	2.01e-5	0.60	0.15
4	3	2.60e-5	0.48	5.38e-5	0.16	0.57
5	4	4.46e-5	0.55	8.09e-5	0.02	0.98
6	5 (R = Me)	1.71e-6	0.23	7.52e-6	0.85	0.02
7	6	7.21e-6	0.37	1.96e-5	0.74	0.09
8	7	1.37e-5	0.44	3.14e-5	0.23	0.30
9	8	2.88e-5	0.43	6.69e-5	0.03	0.72
10	9 (R = 4-Py)	0.69e-6	0.32	2.20e-6	0.16	0.02
11	10	2.21e-5	0.57	3.88e-5	0.01	0.67

^[a]Determined by GC using *n*-dodecane as an internal standard. ^[b]For information pertaining to the calculation of the correction factor CF, please consider the SI. ^[c] $v_{0,\text{corr}} = v_0 / \text{CF}$.

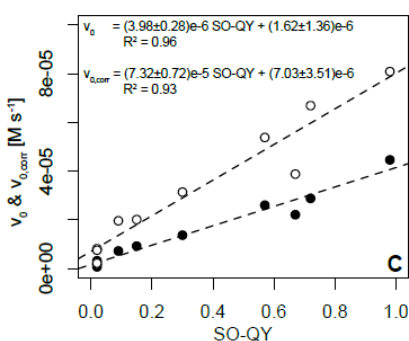
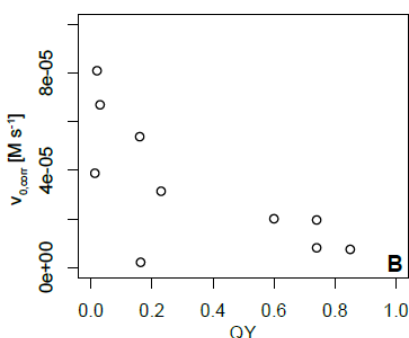
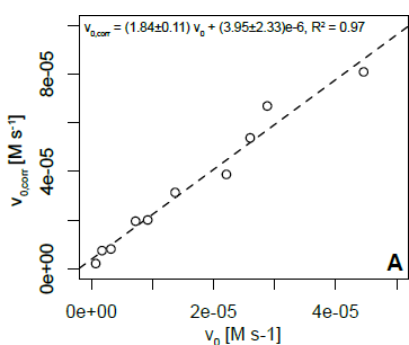


Figure 8. (a) Initial rates v_0 and $v_{0,\text{corr}}$ display a linear dependence, (b) and non-linearly on fluorescence quantum yields. (c) Linear relationships exist between initial rates and singlet oxygen quantum yields Φ_Δ .

Whereas these CF values ranged from 0.23 to 0.57, most were closer to the average value of 0.42 ± 0.10 , indicating that v_0 and $v_{0,\text{corr}}$ correlated linearly (Table 2). This was further substantiated by considering $v_0 \sim v_{0,\text{corr}}$ with a goodness of fit of $R^2 = 0.97$ having been determined (Figure 8a). No linear correlation between fluorescent quantum yields Φ_F and $v_{0,\text{corr}}$ (and v_0) was observed (Figure 8b). However, this is not surprising since the Φ_Δ does not depend linearly on the fluorescence quantum yield. Moreover, the GC-based rates should directly reflect the efficiency of singlet oxygen production ($v_{0,\text{corr}} \sim k_{\text{isc}}$) rather than fluorescence. None the less, singlet oxygen quantum yields should tally with the overall initial rate constant observed for [4+2] cycloadduct formation. Both measurements, v_0 and $v_{0,\text{corr}}$, correlate well with the observed Φ_Δ with excellent goodness of fits ($R^2 = 0.96$ and 0.93 , respectively). The slightly lower value for $v_{0,\text{corr}}$ may be rationalised on the basis of introducing two additional sources of experimental errors when calculating the correction factor: the lamp's emissive profile as well as the chromophore's absorption spectrum. Importantly, however, the high correlation between two experimentally different and independently determined variables (Φ_Δ & v_0) is reassuring. Furthermore, since the photophysical correction factor is not strictly required under the chosen experimental conditions, GC-based initial rates (v_0) may be used for an initial reactivity assessment of singlet oxygen photosensitizers. Determining v_0 by singlet oxygen trapping with anthracene provides a fast and economical way of estimating Φ_Δ . Consequently, it provides an inexpensive and operationally profiling method to assess whether or not a full photophysical characterization of a new photocatalyst is warranted or not.

CONCLUSION

Systematic halogen exchange on photosensitizing BODIPY fluorophores provides unequivocal evidence that both intersystem crossing and singlet oxygen quantum yields scale as the forth power of the atomic number (Z^4). This correlation between Heavy Atom Effect (HAE) and practical photooxidation efficiency can be rapidly and inexpensively assessed by an initial rate approximation requiring only simple GC-based methods ($v_{0,\text{H}} < v_{0,\text{Cl}} < v_{0,\text{Br}} < v_{0,\text{I}}$). Whilst this independent validation of consistency was achieved by correlating GC-based reactivity profiles with a full photophysical analysis, the approach can be easily implemented in research laboratories with standard analytical equipment.

Introduction of halogen substituents in the 2- and 6-position led to the gradual activation of the heavy atom effect in the core structures, as highlighted by consideration of the $k_{\text{nr}}(77\text{K})$ values (these reflecting k_{isc} rates). Whereas substituents with H and Cl led to negligible rates, the installation of Br and I switched on effective intersystem crossing. This was further supported by analysis of singlet oxygen quantum yields determined by infrared emission spectroscopy. Φ_Δ increased in the series $\text{H} < \text{Cl} < \text{Br} < \text{I}$ and values of up to 98% (4) could be observed. Most

Full paper

WILEY-VCH

notably, for double logarithmic plots linear correlations of relative intersystem crossing rates k_{isc}^X / k_{isc}^Y and relative atomic numbers Z^X / Z^Y for the respective substituents with corresponding slopes of approx. 4 were obtained - this being perfectly in line with theoretical predictions for the Heavy Atom Effect. The same observation held true when k_{isc} was substituted by Φ_{Δ} . By trapping singlet oxygen using anthracene in a [4+2] cycloaddition, and monitoring the process by GC, it was possible to characterize the photocatalysts by initial rates (v_0). The trend was fully consistent with the Heavy Atom Effect ($v_{0,H} < v_{0,Cl} < v_{0,Br} < v_{0,I}$). Furthermore, this simple measurement correlated positively and strongly to the Φ_{Δ} determined previously. This inexpensive and operationally simple approach for the comparative analysis of sensitizers eliminates the need for specialized equipment in initial screening evaluations. Given the rapid expansion of organic photochemistry in recent years, it is envisaged that this simple, enabling approach will facilitate photocatalyst profiling.

Experimental Section

General Methods

All reactions were performed under an atmosphere of argon in dried glassware, except when using aqueous reagents. All chemicals were reagent grade and used as supplied unless stated otherwise. All reactions were magnetically stirred. Solvents for extractions and chromatography were technical grade. Extracts were dried over technical grade Na_2SO_4 or MgSO_4 . Analytical thin layer chromatography (TLC) was performed on pre-coated Merck silica gel 60 F₂₅₄ plates (0.25 mm) and visualised by UV, CAM, ninhydrine or KMnO_4 stain. Flash column chromatography was carried out on Fluka silica gel 60 (230-400 mesh). Concentration *in vacuo* was performed at -10 mbar and 40 °C, drying at -10^{-2} mbar and room temperature (caution: some intermediates and products are volatile). ^1H NMR, ^{13}C NMR and ^{19}F NMR spectra were recorded on a Bruker AV 300 MHz, Bruker AV 400 MHz and an Agilent DD2 600 spectrometer. Chemical shifts (δ) are reported in ppm relative to the solvent residual peak. The multiplicities are reported as: s = singlet, d = doublet, t = triplet, q = quartet, sext = sextet, m = multiplet, br = broad. Melting points were measured on a Büchi B540 melting point apparatus. IR spectra were measured on a Perkin-Elmer Spectrum 100 FTIR spectrometer and reported in cm^{-1} . The intensities of the bands are reported as: w = weak, m = medium, s = strong. High-resolution mass spectra (HR ESI and EI MS) were performed by the MS service at the Organic Chemistry Institute of the WWU Münster. HPLC analyses were performed on an Agilent 1260 system.

Absorption spectra were measured on a Varian Cary 5000 double-beam UV-Vis-NIR spectrometer and baseline corrected. Steady-state emission spectra were recorded on a FluoTime300 spectrometer from PicoQuant equipped with a 300 W ozone-free Xe lamp (250-900nm), an excitation monochromator (Czerny-Turner 2.7 nm/mm dispersion, 1200 grooves/mm, blazed at 300 nm), diode lasers (pulse width < 80 ps) operated by a computer-controlled laser driver PDL-820 (repetition rate up to 80 MHz, burst mode for slow and weak decays), two emission monochromators (Czerny-Turner, selectable gratings blazed at 500 nm with 2.7 nm/mm dispersion and 1200 grooves/mm, or blazed at 1250 nm with 5.4 nm/mm dispersion and 600 grooves/mm), and two detectors, namely a PMA Hybrid 40 (transit time spread FWHM < 120 ps, 300 – 720 nm) and a R5509-42 NIR-photomultiplier tube (transit time spread FWHM 1.5 ns, 300-1400 nm) with external cooling (-80 °C) from Hamamatsu. Steady-state spectra and fluorescence lifetimes were recorded in TCSPC mode by a PicoHarp 300 (minimum base resolution 4 ps). Emission and excitation spectra were corrected for source intensity (lamp and grating) and detection arm response (detector and grating) by standard correction curves. Lifetime analysis was performed using the commercial FluoFit

software. The quality of the fit was assessed by minimizing the reduced chi squared function (χ^2) and visual inspection of the weighted residuals and their autocorrelation. Luminescence quantum yields were measured with a Hamamatsu Photonics absolute PL quantum yield measurement system (C9920-02) equipped with a L9799-01 CW Xenon light source (150 W), monochromator, C7473 photonic multi-channel analyzer, integrating sphere, a calibrated quartz Dewar with matching tubes for 77K measurements and employing U6039-05 PLQY measurement software (Hamamatsu Photonics, Ltd., Shizuoka, Japan). All solvents used were of spectroscopic grade.

8-Acetoxyethyl-1,3,5,7-tetramethyl pyrromethene fluoroborate (1)

To a light yellow solution of 2,4-dimethylpyrrole (2.16 mmol, 21.0 mmol) in dry CH_2Cl_2 (100 mL) was added 2-chloro-2-oxoethyl acetate (1.40 mL, 13.0 mmol) dropwise to give an orange solution which was stirred for 4 h. To the resulting dark red solution was added DIPEA (7.30 mL, 43.0 mmol) to give a dark green solution which was stirred for 15 min and then treated with $\text{BF}_3 \cdot \text{OEt}_2$ (5.30 mL, 43.0 mmol) to give a dark red solution. After stirring for 30 min the mixture was washed with water (300 mL). The aqueous layer was extracted with CH_2Cl_2 (2 x 300 mL) and the combined organic layers were dried over Na_2SO_4 and concentrated *in vacuo* to give a dark red oil. This was purified by column chromatography (CH_2Cl_2 : *n*-hex / 1 : 1 \rightarrow 1 : 2) to give an orange, green fluorescent solid (322 mg, 10%). R_f 0.63 (CH_2Cl_2); m.p. 191-193 °C; v_{max} (neat)/ cm^{-1} 2925w, 1753m, 1740m, 1551m, 1508s, 1469m, 1409m, 1389m, 1369m, 1306m, 1189s, 1158s, 1138s, 1072s, 1021s, 969s, 915s, 835s, 810s, 754m, 717s, 662m; ^1H NMR (400 MHz, CDCl_3): δ = 6.08 (2H, s, C^2H and C^6H), 5.29 (2H, s, CH_2), 2.53 (6H, s, C^3CH_3 and C^5CH_3), 2.35 (6H, s, C^1CH_3 and C^7CH_3) and 2.13 (3H, s, $\text{CH}_3\text{CO}_2\text{R}$); ^{13}C NMR (100 MHz, CDCl_3): δ = 170.7 ($\text{CH}_3\text{CO}_2\text{R}$), 156.8 (2C, C^3 and C^5), 141.6 (2C, C^1 and C^7), 133.4 (C^6), 132.8 (2C, C^9 and C^{10}), 122.5 (2C, C^2 and C^6), 58.0 (CH_2), 20.7 ($\text{CH}_3\text{CO}_2\text{R}$), 15.8 (2C, C^1CH_3 and C^7CH_3) and 14.8 (2C, t, $^4J_{\text{CF}}$ 2.4, C^3CH_3 and C^5CH_3); ^{19}F NMR (282 MHz, CDCl_3): δ = -146.4 (Ψ_{q} , $^1J_{\text{BF}}$ 32.5); [m/z (ESI) found: 343.1402 ($\text{M}+\text{Na}^+$), $\text{C}_{16}\text{H}_{19}\text{BF}_2\text{N}_2\text{O}_2\text{Na}$ requires 343.1400]. Data in agreement with the literature values.^[18]

8-Acetoxyethyl-2,6-dichloro-1,3,5,7-tetramethyl pyrromethene fluoroborate (2)

To a brown solution of **1** (16.0 mg, 50.0 μmol) in 1,1,1,3,3,3-hexafluoro-2-propanol (500 μL) was added NCS (14.7 mg, 1.10 mmol) to give a dark purple solution which was stirred for 75 min. A solution of $\text{Na}_2\text{S}_2\text{O}_3 \cdot 5\text{H}_2\text{O}$ (aq., 10% w/w, 1.0 mL) was added and the mixture was extracted with CH_2Cl_2 (2 x 1.0 mL). The combined organic layers were dried over Na_2SO_4 and concentrated *in vacuo* to give a dark purple solid which was purified by column chromatography (CH_2Cl_2 : *n*-pent / 1 : 1) to give a red solid (13.9 mg, 71%). R_f 0.69 (CH_2Cl_2); m.p. 207-210 °C; v_{max} (neat)/ cm^{-1} 2927w, 1733s, 1558s, 1506m, 1470s, 1448m, 1407m, 1391m, 1377m, 1357s, 1319m, 1220s, 1179s, 1128s, 1113s, 1082s, 1067s, 1055s, 1030s, 991s, 917s, 895s, 883s, 839m, 720s, 678m, 662m, 656m; ^1H NMR (600 MHz, CDCl_3): δ = 5.30 (2H, s, CH_2), 2.57 (6H, s, C^3CH_3 and C^5CH_3), 2.36 (6H, s, C^1CH_3 and C^7CH_3) and 2.14 (3H, s, $\text{CH}_3\text{CO}_2\text{R}$); ^{13}C NMR (150 MHz, CDCl_3): δ = 170.5 ($\text{CH}_3\text{CO}_2\text{R}$), 153.9 (2C, C^3 and C^5), 136.3 (2C, C^1 and C^7), 134.3 (C^6), 131.4 (2C, C^9 and C^{10}), 123.7 (2C, C^2 and C^6), 57.9 (CH_2), 20.7 ($\text{CH}_3\text{CO}_2\text{R}$), 13.1 (2C, C^1CH_3 and C^7CH_3) and 12.8 (2C, t, $^4J_{\text{CF}}$ 2.4, C^3CH_3 and C^5CH_3); ^{19}F NMR (564 MHz, CDCl_3): δ = -146.4 (Ψ_{q} , $^1J_{\text{BF}}$ 31.5); [m/z (ESI) found: 411.0622 ($\text{M}+\text{Na}^+$), $\text{C}_{16}\text{H}_{17}\text{BCl}_2\text{F}_2\text{N}_2\text{O}_2\text{Na}$ requires 411.0626]. Data in agreement with the literature values.^[18]

8-Acetoxyethyl-2,6-dibromo-1,3,5,7-tetramethyl pyrromethene fluoroborate (3)

To a brown solution of **1** (16.0 mg, 50.0 μmol) in 1,1,1,3,3,3-hexafluoro-2-propanol (500 μL) was added NBS (19.6 mg, 1.10 mmol) to give a dark purple solution which was stirred for 15 min. A solution of $\text{Na}_2\text{S}_2\text{O}_3 \cdot 5\text{H}_2\text{O}$ (aq., 10% w/w, 1.0 mL) was added and the mixture was extracted with CH_2Cl_2 (2 x 1.0 mL). The combined organic layers were dried over Na_2SO_4 and concentrated *in vacuo* to give a dark purple solid which was purified by column chromatography (CH_2Cl_2 : *n*-pent / 1 : 1) to give a red solid (12.1 mg, 51%). R_f 0.72 (CH_2Cl_2); m.p. 235-238 °C; v_{max} (neat)/ cm^{-1}

2925w, 1734m, 1556s, 1501m, 1464m, 1447m, 1404m, 1388m, 1376m, 1352s, 1313m, 1217s, 1173s, 1126s, 1098s, 1081s, 1048s, 1028s, 987s, 917s, 888s, 875s, 838m, 719s, 678m, 658m; ¹H NMR (600 MHz, CDCl₃): δ = 5.31 (2H, s, CH₂), 2.59 (6H, s, C³CH₃ and C⁵CH₃), 2.38 (6H, s, C¹CH₃ and C⁷CH₃) and 2.14 (3H, s, CH₃CO₂R); ¹³C NMR (150 MHz, CDCl₃): δ = 170.5 (CH₃CO₂R), 155.3 (2C, C³ and C⁵), 138.9 (2C, C¹ and C⁷), 133.9 (C⁶), 131.9 (2C, C⁹ and C¹⁰), 113.1 (2C, C² and C⁶), 58.1 (CH₂), 20.7 (CH₃CO₂R), 15.0 (2C, C¹CH₃ and C⁷CH₃) and 14.1 (2C, t, ⁴J_{CF} 2.6, C³CH₃ and C⁵CH₃); ¹⁹F NMR (564 MHz, CDCl₃): δ = -146.1 (Ψq, ¹J_{BF} 31.6); [m/z (ESI) found: 500.9591 (M+Na)⁺, C₁₆H₁₇BBF₂N₂O₂Na requires 500.9595]. Data in agreement with the literature values.^[13b]

8-Acetoxyethyl-2,6-diiodo-1,3,5,7-tetramethyl pyrromethene fluoroborate (4)

To an orange suspension of **1** (157 mg, 491 μmol) in EtOH (50 mL) under air was added iodine (249 mg, 981 μmol) and HIO₃ (173 mg, 981 μmol) to give a dark red suspension which was stirred for 24 h. Water (50 mL) was added and the mixture was extracted with CH₂Cl₂ (2 x 50 mL). The combined organic layers were washed with a Na₂S₂O₃·5H₂O solution (aq., 10% w/w, 100 mL) and the aqueous layer was back-extracted with CH₂Cl₂ (50 mL). The combined organic layers were dried over Na₂SO₄ and concentrated *in vacuo*. Purification by column chromatography (CH₂Cl₂: c-Hex / 1 : 1, dry loading) afforded **4** as a red solid (208 mg, 74%). R_f 0.83 (CH₂Cl₂); m.p. 185–188 °C; v_{max} (neat)/cm⁻¹ 3468w, 2921w, 1737s, 1544s, 1489m, 1439m, 1398m, 1374m, 1345s, 1307m, 1217s, 1172s, 1123s, 1077s, 1044s, 1031s, 984s, 917s, 837s, 741m, 719s, 677s, 656s; ¹H NMR (400 MHz, CDCl₃): δ = 5.30 (2H, s, CH₂), 2.63 (6H, s, C³CH₃ and C⁵CH₃), 2.39 (6H, s, C¹CH₃ and C⁷CH₃) and 2.14 (3H, s, CH₃CO₂R); ¹³C NMR (100 MHz, CDCl₃): δ = 170.5 (CH₃CO₂R), 158.1 (2C, C³ and C⁵), 143.6 (2C, C¹ and C⁷), 132.9 (C⁶), 132.7 (2C, C⁹ and C¹⁰), 87.4 (2C, C² and C⁶), 58.4 (CH₂), 20.7 (CH₃CO₂R), 18.3 (2C, C¹CH₃ and C⁷CH₃) and 16.5 (2C, t, ⁴J_{CF} 2.6, C³CH₃ and C⁵CH₃); ¹⁹F NMR (282 MHz, CDCl₃): δ = -145.6 (Ψq, ¹J_{BF} 31.8); [m/z (ESI) found: 594.9329 (M+Na)⁺, C₁₆H₁₇BF₂N₂O₂Na requires 594.9333]. Data in agreement with the literature values.^[13a]

1,3,5,7,8-pentamethyl pyrromethene fluoroborate (5)

A light orange solution of 2,4-dimethylpyrrole (1.90 mL, 18.5 mmol) in dry CH₂Cl₂ (100 mL) was cooled to 0 °C then acetyl chloride (789 μL, 11.1 mmol) was added dropwise to give a yellow solution which was allowed to warm to rt and stirred for 26 h. To the resulting dark red solution was added DIPEA (6.42 mL, 36.9 mmol) and the solution was stirred for 15 min before the addition of BF₃·OEt₂ (4.56 mL, 36.9 mmol). The dark red solution was stirred for 30 min, a saturated NaHCO₃ solution (aq., 200 mL) was added and the mixture was extracted with CH₂Cl₂ (3 x 200 mL). The combined organic layers were dried over Na₂SO₄ and concentrated *in vacuo* to give a dark red solid which was purified by column chromatography (CH₂Cl₂: c-hex / 1 : 1) to give a bright orange solid (627 mg, 26%). R_f 0.33 (CH₂Cl₂: c-hex / 1 : 1); m.p. 260–262 °C; v_{max} (neat)/cm⁻¹ 2985w, 1721w, 1667w, 1554m, 1531m, 1500m, 1435m, 1400s, 1362m, 1303m, 1227w, 1188s, 1159s, 1128m, 1074s, 1056s, 1026s, 996m, 972s, 840m, 806s, 764m, 747m, 723s, 698m, 675m; ¹H NMR (400 MHz, CDCl₃): δ = 6.04 (2H, s, C²H and C⁶H), 2.55 (3H, s, C⁸CH₃), 2.51 (6H, s, C³CH₃ and C⁵CH₃) and 2.40 (6H, s, C¹CH₃ and C⁷CH₃); ¹³C NMR (100 MHz, CDCl₃): δ = 153.7 (2C, C³ and C⁵), 141.6 (C⁶), 141.1 (2C, C¹CH₃ and C⁷CH₃), 132.2 (2C, C⁹ and C¹⁰), 121.4 (2C, C² and C⁶), 17.4 (2C, C¹CH₃ and C⁷CH₃), 16.5 (C, C⁸CH₃) and 14.6 (2C, t, ⁴J_{CF} 2.4, C³CH₃ and C⁵CH₃); ¹⁹F NMR (282 MHz, CDCl₃): δ = -146.7 (Ψq, ¹J_{BF} 32.9); [m/z (ESI) found: 285.1348 (M+Na)⁺, C₁₄H₁₇BF₂N₂Na requires 285.1345]. Data in agreement with the literature values.^[19]

2,6-dichloro-1,3,5,7,8-pentamethyl pyrromethene fluoroborate (6)

To a clear orange solution of **5** (30.0 mg, 115 μmol) in 1,1,1,3,3,3-hexafluoro-2-propanol (1.2 mL) was added NCS (33.8 mg, 252 μmol) to give an orange suspension. After 1 h CH₂Cl₂ (500 μL) was added and the mixture was stirred for 30 min before it was diluted with more CH₂Cl₂ (5.0 mL) and washed with a solution of Na₂S₂O₃·5H₂O (aq., 10% w/w, 5.0 mL). The aqueous layer was extracted with CH₂Cl₂ (5.0 mL), the

combined organic layers were dried over Na₂SO₄ and concentrated *in vacuo* to give a red solid. Purification by column chromatography (CH₂Cl₂: n-pent / 1 : 1) gave a red solid (21.1 mg, 55%). R_f 0.53 (CH₂Cl₂: c-hex / 1 : 1); m.p. 269–272 °C; v_{max} (neat)/cm⁻¹ 2927w, 1548m, 1501m, 1470m, 1447m, 1404m, 1384m, 1350m, 1313m, 1226m, 1192s, 1131m, 1110s, 1065s, 1052s, 1026m, 997s, 903m, 891m, 829m, 723m, 695m, 677m, 658m; ¹H NMR (600 MHz, CDCl₃): δ = 2.62 (3H, s, C⁸CH₃), 2.55 (6H, s, C³CH₃ and C⁵CH₃) and 2.42 (6H, s, C¹CH₃ and C⁷CH₃); ¹³C NMR (150 MHz, CDCl₃): δ = 150.9 (2C, C³ and C⁵), 142.4 (C⁶), 136.0 (2C, C¹ and C⁷), 130.6 (2C, C⁹ and C¹⁰), 122.5 (2C, C² and C⁶), 17.2 (C⁸CH₃), 14.7 (2C, C¹CH₃ and C⁷CH₃) and 12.5 (2C, t, ⁴J_{CF} 2.4, C³CH₃ and C⁵CH₃); ¹⁹F NMR (564 MHz, CDCl₃): δ = -146.7 (Ψq, ¹J_{BF} 31.3); [m/z (ESI) found: 353.0567 (M+Na)⁺, C₁₄H₁₅BCl₂F₂N₂Na requires 353.0571]. Data in agreement with the literature values.^[20]

2,6-dibromo-1,3,5,7,8-pentamethyl pyrromethene fluoroborate (7)

To a clear orange solution of **5** (30.0 mg, 115 μmol) in 1,1,1,3,3,3-hexafluoro-2-propanol (1.2 mL) was added NBS (44.9 mg, 252 μmol) to give a dark red suspension. After 20 min it was diluted with CH₂Cl₂ (5.0 mL) and washed with a solution of Na₂S₂O₃·5H₂O (aq., 10% w/w, 5.0 mL). The aqueous layer was extracted with CH₂Cl₂ (5.0 mL), the combined organic layers were dried over Na₂SO₄ and concentrated *in vacuo* to give a red solid. Purification by column chromatography (CH₂Cl₂: n-pent / 1 : 1) gave a red solid (20.4 mg, 42%). R_f 0.59 (CH₂Cl₂: c-hex / 1 : 1); m.p. 236–239 °C; v_{max} (neat)/cm⁻¹ 2922w, 1543m, 1466m, 1446m, 1400m, 1382m, 1345s, 1309m, 1224m, 1189s, 1130m, 1100s, 1067s, 1046s, 993s, 897m, 827m, 721s; ¹H NMR (600 MHz, CDCl₃): δ = 2.63 (3H, s, C⁸CH₃), 2.57 (6H, s, C³CH₃ and C⁵CH₃) and 2.44 (6H, s, C¹CH₃ and C⁷CH₃); ¹³C NMR (150 MHz, CDCl₃): δ = 152.4 (2C, C³ and C⁵), 142.1 (C⁶), 138.5 (2C, C¹ and C⁷), 131.4 (2C, C⁹ and C¹⁰), 111.8 (2C, C² and C⁶), 17.5 (C⁸CH₃), 16.6 (2C, C¹CH₃ and C⁷CH₃) and 13.8 (2C, t, ⁴J_{CF} 2.6, C³CH₃ and C⁵CH₃); ¹⁹F NMR (564 MHz, CDCl₃): δ = -146.3 (Ψq, ¹J_{BF} 31.9); [m/z (ESI) found: 442.9524 (M+Na)⁺, C₁₄H₁₅BBF₂N₂Na requires 442.9540]. Data in agreement with the literature values.^[13b]

2,6-diiodo-1,3,5,7,8-pentamethyl pyrromethene fluoroborate (8)

To a bright orange suspension of **5** in EtOH (50 mL) under air was added iodine (254 mg, 1.00 mmol) and HIO₃ (176 mg, 1.00 mmol) to give a dark orange suspension which was stirred for 16 h. A solution of Na₂S₂O₃·5H₂O (aq., 10% w/w, 100 mL) was added and the mixture was extracted with CH₂Cl₂ (2 x 100 mL). The combined organic layers were dried over Na₂SO₄ and concentrated *in vacuo*. Purification by column chromatography (CH₂Cl₂: c-Hex / 1 : 1, dry loading) afforded **8** as a bright red solid (217 mg, 84%). R_f 0.67 (CH₂Cl₂: c-hex / 1 : 1); m.p. 220–222 °C; v_{max} (neat)/cm⁻¹ 2965w, 2091w, 1536m, 1442m, 1379m, 1340m, 1305m, 1223w, 1188m, 1092s, 1066s, 988s, 826m, 720s; ¹H NMR (600 MHz, CDCl₃): δ = 2.62 (3H, s, C⁸CH₃), 2.61 (6H, s, C³CH₃ and C⁵CH₃) and 2.46 (6H, s, C¹CH₃ and C⁷CH₃); ¹³C NMR (150 MHz, CDCl₃): δ = 155.2 (2C, C³ and C⁵), 143.1 (2C, C¹ and C⁷), 141.3 (C⁶), 132.3 (2C, C⁹ and C¹⁰), 85.9 (2C, C² and C⁶), 20.0 (2C, C¹CH₃ and C⁷CH₃), 18.0 (C⁸CH₃) and 16.2 (2C, t, ⁴J_{CF} 2.7, C³CH₃ and C⁵CH₃); ¹⁹F NMR (282 MHz, CDCl₃): δ = -145.9 (Ψq, ¹J_{BF} 32.0); [m/z (ESI) found: 539.9283 (M+Na)⁺, C₁₄H₁₅BF₂N₂Na requires 539.9278]. Data in agreement with the literature values.^[13b]

8-(4'-pyridyl)-1,3,5,7-tetramethyl pyrromethene fluoroborate (9)

A colourless solution of 2,4-dimethylpyrrole (500 μL, 4.86 mmol) and 4-pyridinecarboxaldehyde (218 μL, 2.31 mmol) in dry CH₂Cl₂ (20 mL) was treated with TFA (13 μL) and stirred for 50 min to give a clear, bright orange solution. A suspension of DDQ (524 mg, 2.31 mmol) in dry CH₂Cl₂ (5 mL) was added to give a dark red solution which was stirred for 50 min. NEt₃ (5 mL) was added and the resulting dark green solution was stirred for 30 min before BF₃·OEt₂ (5 mL) was added. The obtained dark red solution was stirred for 2 h, then water (100 mL) was added. The mixture was extracted with CH₂Cl₂ (100 mL), the organic layer was dried over Na₂SO₄ and concentrated *in vacuo* to give a dark red oil. This was purified by column chromatography (EtOAc: c-hex / 1 : 1) to give a red, green fluorescent solid (94.8 mg, 13%). R_f 0.39 (EtOAc: c-hex /

1 : 1); m.p. 218–221 °C; ν_{\max} (neat)/cm⁻¹ 2924w, 1599w, 1537s, 1505s, 1464m, 1435m, 1404m, 1368m, 1360m, 1303s, 1263m, 1217w, 1180s, 1152s, 1120m, 1073s, 1051s, 963s, 827m, 809s, 766s, 718s, 671; ¹H NMR (400 MHz, CDCl₃): δ = 8.79–8.75 (2H, m, C²H and C⁶H), 7.32–7.29 (2H, m, C³H and C⁵H), 6.00 (2H, s, C²H and C⁶H), 2.55 (6H, s, C³CH₃ and C⁵CH₃) and 1.40 (6H, s, C¹CH₃ and C⁷CH₃); ¹³C NMR (100 MHz, CDCl₃): δ = 156.6 (2C, C³ and C⁵), 150.7 (2C, C² and C⁶), 143.8 (C⁹), 142.8 (2C, C¹ and C⁷), 137.7 (C⁴), 130.5 (2C, C⁹ and C¹⁰), 123.5 (2C, C³ and C⁵), 121.9 (2C, C² and C⁶), 14.77 (2C, t, ⁴J_{CF} 2.2, C³CH₃ and C⁵CH₃) and 14.75 (2C, C¹CH₃ and C⁷CH₃); ¹⁹F NMR (282 MHz, CDCl₃): δ = -146.3 (Ψ _q, ¹J_{BF} 32.5); [*m/z* (ESI) found: 326.1633 (M+H)⁺, C₁₈H₁₉BF₂N₃O requires 326.1635]. Data in agreement with the literature values.^[21]

2,6-diiodo-8-(4'-pyridyl)-1,3,5,7-tetramethyl pyrromethene fluoroborate (10)

To a dark red solution of **9** (14.0 mg, 43.1 μ mol) in 1,1,1,3,3,3-hexafluoro-2-propanol (370 μ L) was added NIS (20.1 mg, 89.1 μ mol) and the mixture was stirred for 10 min. A solution of Na₂S₂O₃·5H₂O (aq., 10% w/w, 10 mL) was added and the mixture was extracted with CH₂Cl₂ (3 x 10 mL). The combined organic layers were dried over Na₂SO₄ and concentrated *in vacuo* to give a red solid which was purified by column chromatography (EtOAc : c-hex / 1 : 4, dry loading) to give a dark red solid (23.4 mg, 94%). R_f 0.65 (EtOAc : c-hex / 1 : 1); m.p. 220–223 °C; ν_{\max} (neat)/cm⁻¹ 2921w, 2852w, 2313w, 2094w, 1888w, 1709w, 1636w, 1602w, 1526s, 1444m, 1397m, 1344m, 1306m, 1270w, 1167s, 1119s, 1060s, 986s, 917s, 867m, 823m, 794m, 761s, 718s, 705s, 659; ¹H NMR (400 MHz, CDCl₃): δ = 8.84 (2H, d, ³J 5.4, C²H and C⁶H), 7.36 (2H, d, ³J 5.9, C³H and C⁵H), 2.65 (6H, s, C³CH₃ and C⁵CH₃) and 1.42 (6H, s, C¹CH₃ and C⁷CH₃); ¹³C NMR (100 MHz, CDCl₃): δ = 158.2 (2C, C³ and C⁵), 150.1 (2C, C²H and C⁶H), 144.9 (2C, C¹ and C⁷), 144.6 (C⁴), 136.7 (C⁹), 130.3 (2C, C⁹ and C¹⁰), 123.7 (2C, C³H and C⁵H), 86.6 (2C, C² and C⁶), 17.5 (2C, C¹CH₃ and C⁷CH₃) and 16.3 (2C, t, ⁴J_{CF} 2.4, C³CH₃ and C⁵CH₃); ¹⁹F NMR (282 MHz, CDCl₃): δ = -145.6 (Ψ _q, ¹J_{BF} 32.0); [*m/z* (ESI) found: 577.9571 (M+H)⁺, C₁₈H₁₇BF₂N₃ requires 577.9567]. Data in agreement with the literature values.^[19]

9,10-dihydro-9,10-epidioxyanthracene

A 10 mL Schlenk flask was set under an oxygen atmosphere and loaded with a solution of anthracene (17.8 mg, 100 μ mol), the appropriate sensitizer (1 μ mol) and *n*-dodecane (22.7 μ L, 100 μ mol) in CDCl₃ (1.0 mL). The CDCl₃ was washed with a Na₂S₂O₃ solution aq., 10% prior to use. The solution was irradiated with a halogen lamp (400 W, as Schwabe (Art.-Nr. 46012)) at 30 cm distance through a UV filter (hama, UV 390 Protect Filter, 52 mm) while stirring at 500 rpm. Aliquots (~10 μ L) were taken at the indicated times, diluted with CH₂Cl₂ and kept in the dark until analysed by gas chromatography (method: 40 °C to 180 °C at 10 °C per minute, then 180 °C isothermal; t_R: *n*-dodecane: 10.6 min; anthracene: 35.3 min; endoperoxide decomposes). Irradiation was stopped after 3 h, the solution was concentrated *in vacuo* at 30 °C and the residue was purified by column chromatography to give a white solid. R_f 0.23 (CH₂Cl₂ : *n*-pentane / 1 : 2); ν_{\max} (neat)/cm⁻¹ 2968w, 1668w, 1600w, 1461m, 1316m, 1241w, 1172w, 933w, 867m, 808m, 767s, 752s, 714m; ¹H NMR (400 MHz, CDCl₃): δ = 7.45–7.39 (4H, m, C¹H, C⁴H, C⁵H and C⁸H), 7.32–7.26 (4H, m, C²H, C³H, C⁶H and C⁷H) and 6.03 (2H, s, C⁹H and C¹⁰H); ¹³C NMR (100 MHz, CDCl₃): δ = 138.2 (4C, C^{4a}, C^{5a}, C^{8a} and C^{9a}), 128.1 (4C, C², C³, C⁶ and C⁷), 123.7 (4C, C¹, C⁴, C⁵ and C⁸), and 79.5 (2C, C⁹ and C¹⁰); [*m/z* (ESI) found: 233.0579 (M+Na)⁺, C₁₄H₁₀O₂Na requires 233.0578]. Data in agreement with the literature values.^[22]

Acknowledgements

We acknowledge generous financial support from the WWU Münster, the Deutsche Forschungsgemeinschaft (SFB 858, and Excellence Cluster EXC 1003 "Cells in Motion – Cluster of Excellence"), the Alexander von

Humboldt Foundation and the Swiss National Science Foundation (NS, P300P2_161070).

Keywords: halogens • heavy atom effect • physical organic chemistry • reaction profiling

- [1] For selected reviews on the generation and application of singlet oxygen see (a) M. C. DeRosa, R. J. Crutchley, *Coord. Chem. Rev.* **2002**, 233–234, 351–371; (b) C. Schweitzer, R. Schmidt, *Chem. Rev.* **2003**, 103, 1685–1757; (c) E. L. Clennan, A. Pace, *Tetrahedron* **2005**, 61, 6665–6691; (d) N. Hoffmann, *Chem. Rev.* **2008**, 108, 1052–1103; (e) P. R. Ogilby, *Chem. Soc. Rev.* **2010**, 39, 3181–3209.
- [2] B. M. Trost, *Science* **1991**, 254, 1471–1477.
- [3] For a review on sustainable catalytic oxidation see: F. Cavani, H.-J. Teles, *ChemSusChem* **2009**, 2, 508–534.
- [4] (a) D. E. J. G. J. Dolmans, D. Fukumura, R. K. Jain, *Nature Reviews Cancer* **2003**, 3, 380–387; (b) A. Kamkaew, S. H. Lim, H. B. Lee, L. V. Kiew, L. Y. Chung, K. Burgess, *Chem. Soc. Rev.* **2013**, 42, 77–88.
- [5] (a) T. Montagon, M. Tofi, G. Vassilikogiannakis, *Acc. Chem. Res.* **2008**, 41, 1001–1011; (b) A. A. Ghogare, A. Greer, *Chem. Rev.* **2016**, DOI: 10.1021/acs.chemrev.5b00726.
- [6] N. J. Turro, V. Ramamurthy and J. C. Scaiano, *Modern Molecular Photochemistry of Organic Molecules*, University Science Books, Sausalito, 2010.
- [7] For selected reviews see (a) T. P. Yoon, M. A. Ischay, J. Du, *Nat. Chem.* **2010**, 2, 527–532; (b) J. M. R. Narayanam, C. R. J. Stephenson, *Chem. Soc. Rev.* **2011**, 40, 102–113; (c) C. K. Prier, D. A. Rankic, D. W. C. MacMillan, *Chem. Rev.* **2013**, 113, 5322–5363; (d) T. Koike, M. Akita *Synlett* **2013**, 24, 2492–2505; (e) D. A. Nicewicz, T. M. Nguyen, *ACS Catal.* **2014**, 4, 355–360; (f) N. A. Romero, D. A. Nicewicz, *Chem. Rev.* **2016**, DOI: 10.1021/acs.chemrev.6b00057.
- [8] For a review see: A. Loudet, K. Burgess, *Chem. Rev.* **2007**, 107, 4891–4932.
- [9] (a) J. C. Koziar, D. O. Cowan, *Acc. Chem. Res.* **1978**, 11, 334–341; (b) S. Banfi, G. Nasini, S. Zaza, E. Caruso, *Tetrahedron* **2013**, 69, 4845–4856; (c) T. Yogo, Y. Urano, Y. Ishitsuka, F. Maniwa, T. Nagano, *J. Am. Chem. Soc.* **2005**, 127, 12162–12163; (d) R. P. Sabatini, T. M. McCormick, T. Lazarides, K. C. Wilson, R. Eisenberg, D. W. McCamant *J. Phys. Chem. Lett.* **2011**, 2, 223–227; (e) M. J. Ortiz, A. R. Agarrabeitia, G. Duran-Sampedro, J. Bañuelos Prieto, T. A. Lopez, W. A. Massad, H. A. Montejano, N. A. García, I. Lopez Arbeloa, *Tetrahedron* **2012**, 68, 1153–1162.
- [10] Upon irradiation, organic chromophores reach an excited singlet state which generally possesses a short lifetime. In order to efficiently transfer energy, intersystem crossing (ISC) to a triplet excited state which is longer lived has to occur. The probability of ISC can be enhanced by heavy atoms and it is directly related to the atomic number of such substituents. This phenomenon is known as the Heavy Atom Effect (HAE).
- [11] For selected synthetic routes see (a) L. Jiao, W. Pang, J. Zhou, Y. Wei, X. Mu, G. Bai, E. Hao, *J. Org. Chem.* **2011**, 76, 9988–9996; (b) L. Wang J.-W. Wang, A.-j. Cui, X.-X. Cai, Y. Wan, Q. Chen, M.-Y. He, W. Zhang, *W. RSC Adv.* **2013**, 3, 9219–9222.
- [12] M. C. DeRosa, R. J. Crutchley, *Coord. Chem. Rev.* **2002**, 233, 351–371.
- [13] For recent systematic studies of the factors governing singlet oxygen production in BODIPY derivatives see (a) N. Epelde-Elezcano, V. Martínez-Martínez, E. Peña-Cabrera, C. F. A. Gómez-Durán, I. López Arbeloa, S. Lacombe, *RSC Adv.* **2016**, 6, 41991–41998; (b) A. M. Durantini, L. E. Greene, R. Lincoln, S. R. Martínez, G. Cosa, *J. Am. Chem. Soc.* **2016**, 138, 1215–1225.
- [14] (a) H. L. Wang, C. H. Du, Y. Pu, R. Adur, P. C. Hammel and F. Y. Yang, *Phys. Rev. Lett.* **2014**, 112, 197201; (b) C. Du, H. Wang, F. Y. Yang, P. C. Hammel, *Phys. Rev. B* **2014**, 90, 140407; (c) Y. Tserkovnyak, A. Brataas, G. E. W. Bauer, B. I. Halperin, *ChemInform* **2005**, 36(6).
- [15] D. D. Sarma, *Proc. Indian Acad. Sci. - Chem. Sci.* **1981**, 90, 19–26.
- [16] Valeur, B. *Molecular Fluorescence: Principles and Applications*. (WILEY-VCH Verlag, 2001).

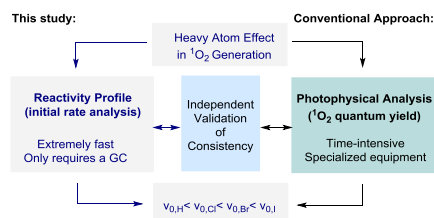
- [17] D. A. Fernández, J. Awruch, L. E. Dixelio, *Photochem. Photobiol.* **1996**, 63, 784-792.
- [18] K. Krumova, G. Cosa, *J. Am. Chem. Soc.* **2010**, 132, 17560-17569.
- [19] S. Choi, J. Bouffard, Y. Kim *Chem. Sci.* **2014**, 5, 751-755.
- [20] G. Duran-Sampedro, A. R. Agarrabeitia, I. Garcia-Moreno, A. Costela, J. Bañuelos, T. Arbeloa, I. López Arbeloa, J. Luis Chiara, M. J. Ortiz *Eur. J. Org. Chem.* **2012**, 6335-6350.
- [21] A. Barba-Bon, A. M. Costero, S. Gil, A. Harriman, F. Sancenón, *Chem. Eur. J.* **2014**, 20, 6339-6347.
- [22] J. Carney, R. Hammer, M. Hulce, C. Lomas, D. Miyashiro, *Synthesis* **2012**, 44, 2560-2566.

WILEY-VCH

Accepted Manuscript

Text for Table of Contents

A facile GC-based method to assess catalyst performance has been developed, and validated using a focused set of halogenated BODIPY scaffolds. An initial rate approximation was applied to a model transformation and follows the HAE trend ($v_{0,H} < v_{0,Cl} < v_{0,Br} < v_{0,I}$). This approach was corroborated by complementary determination of absolute singlet oxygen and photoluminescent quantum yields and time-resolved luminescence decays.



Catalyst profiling, photocatalysis*

Yannick P. Rey, Dario G. Abradelo, Nico Santschi, Cristian A. Strassert, and Ryan Gilmour

Page No. – Page No.

Title